



Idiopathic ventricular arrhythmias arising from the posterior septum of tricuspid and mitral annuli: comparison of electrocardiographic characteristics and outcomes of catheter ablation

Eiji Sato^{1,2} · Tetsuo Yagi¹ · Akihiko Ishida¹ · Yoshiaki Mibiki¹ · Yoshihiro Yamashina¹ · Hirokazu Sato¹ · Takashi Nakagawa¹ · Kosuke Aoki¹ · Keisuke Suzuki¹ · Izutsu Takuma¹ · Tomoyuki Yambe²

Received: 6 March 2018 / Accepted: 20 September 2018 / Published online: 2 October 2018
© Springer Science+Business Media, LLC, part of Springer Nature 2018

Abstract

Purpose Ventricular arrhythmia (VA) arising from the tricuspid annulus in the posterior septum (PS) (TAPS-VA) has similar electrocardiographic characteristics as VA arising from the mitral annulus in the PS (MAPS-VA) because the two locations are adjacent. We examined the electrocardiographic characteristics that differentiate MAPS-VA from TAPS-VA and the efficacy of catheter ablation.

Methods We studied 13 patients whose VAs were successfully ablated in the TAPS ($n = 7$) and MAPS ($n = 6$).

Results QRS morphologies of both groups were characterized by left and right bundle block morphologies in lead V1, superior axis deviation, and precordial transition at \leq lead V3 in nine patients. Compared with TAPS-VA, MAPS-VA had (1) R < S wave in lead II, (2) precordial transition in lead V2, (3) s-wave in lead V6, and (4) slurred initial part of the QRS complex in the precordial leads, e.g., [4a] pseudo delta wave ≥ 34 ms, [4b] intrinsicoid deflection time ≥ 85 ms, and [4c] maximum deflection index ≥ 0.55 . Patients who met ≥ 2 of (1)–(3) and any of [4a]–[4c] could be classified as having MAPS-VA, with a sensitivity and specificity of 100%. VA recurred in one patient in the TAPS group during the median follow-up of 7 (interquartile range 6 to 15.5) months.

Conclusions VA arising from the PS has superior axis deviation, and left and right bundle block morphologies with relatively early precordial transition. MAPS-VA can be differentiated from TAPS-VA based on electrocardiographic characteristics. This study provides useful information for treatment involving catheter ablation for VA arising from the PS.

Keywords Ventricular arrhythmia · Tricuspid annulus · Mitral annulus · Posterior septum · Catheter ablation · ECG

1 Introduction

Idiopathic ventricular arrhythmia (VA) is VA that occurs in patients without underlying heart disease, and it may originate from various sites in the ventricle [1, 2]. The most common site for idiopathic VA is the right ventricular outflow tract, although VA may also occur in the left ventricular inferior septal region, para-Hisian region, tricuspid annulus (TA) [3, 4], mitral annulus (MA) [5–7], and rarely, the cardiac crux on the epicardium side [8, 9]. VA arising from the posterior-

superior process (PSP) of the left ventricle (LV) has been reported in very rare cases [10].

Twelve-lead electrocardiograms (ECG) of the VA originating in the ventricular outflow tract show a waveform indicating a left bundle branch block (LBBB) and inferior axis deviation. Since the left ventricular outflow tract is close to the right ventricular outflow tract anatomically, various electrocardiographic methods for differentiating ventricular outflow VA have been developed [11–13]. As the TA is close to the MA at the ventricular posterior septum, VA originating from the TA in the posterior septal region (TAPS-VA) and that originating from the MA in the posterior septal region (MAPS-VA) show similar ECG waveforms. It has been reported that TAPS-VA shows superior axis deviation with precordial transition in lead V2 or V3 [3, 4], and MAPS-VA shows superior axis deviation with precordial transition in lead V1 or V2 [5, 6]. Both types of VA have a relatively early precordial transition; however, there is no report comparing the ECG characteristics of TAPS-VA and MAPS-VA. This

✉ Tetsuo Yagi
tetsuo.yagi@nifty.com

¹ Division of Cardiology, Sendai City Hospital, Taihaku-ku, Asutonagamachi1-1-1, Sendai, Miyagi 982-8502, Japan

² Department of Medical Engineering and Cardiology, Institute of Development, Aging and Cancer, Tohoku University, Sendai, Japan

study aimed to compare TAPS-VA and MAPS-VA directly to determine their ECG characteristics and the efficacy of catheter ablation.

2 Methods

2.1 Study population

Among 175 consecutive patients who underwent radiofrequency catheter ablation (RFCA) for idiopathic VA at Sendai City Hospital between 2008 and 2015, 13 patients with VA originating from the atrioventricular (AV) annulus in the posterior septal region were included in this study. Of the 13 patients, 7 underwent successful RFCA for TAPS-VA (TAPS group), and 6 underwent successful RFCA for MAPS-VA (MAPS group). Age, sex, symptoms, the medical history, presence of syncopal episode, medication, and left ventricular ejection fraction were recorded for all patients. To evaluate the incidence of coronary artery disease, all patients underwent at least one of the following tests preoperatively: echocardiography, coronary angiography, coronary computed tomography (CT), myocardial perfusion scintigraphy, or cardiac magnetic resonance imaging (MRI).

2.2 ECG analysis

The 12-lead ECGs obtained during VA before ablation were analyzed, with a focus on the following characteristics: form of VA, LBBB or right bundle branch block (RBBB) morphology in lead V1, frontal plane axis, precordial transition, QRS duration, R/S ratio in lead II, lead II/III amplitude ratio, lead aVR/aVL amplitude ratio, and s-wave in lead V6. To assess the slurred initial part of the QRS complex in the precordial leads, we measured the following four items described by Berruezo et al. [14] and Daniels et al. [15]: the pseudo delta wave, intrinsicoid deflection time, shortest RS complex, and maximum deflection index (MDI). These measurements were based on the measurement criteria in the aforementioned articles. All measurements were conducted at a paper speed of 50 mm/s by two independent electrophysiologists who used a digital caliper that measured in increments of 1 ms. Capital letters (Q, R, and S) were used to refer to relatively high amplitude waves (>0.5 mV), and small letters (q, r, and s) were used to refer to relatively low amplitude waves (<0.5 mV).

2.3 Electrophysiological study—mapping and ablation

The patients discontinued all anti-arrhythmic drugs before initiation of the electrophysiological study (EPS) and RFCA. All patients underwent EPS and RFCA using a three-dimensional

(3D) electroanatomical mapping system (CARTO XP, CARTO 3; Biosense-Webster, Diamond Bar, CA). Multiple electrode catheters were inserted from the femoral vein and placed in the coronary sinus (CS), His bundle, and right ventricular (RV) apex. When VA was not observed, isoproterenol at 1–7 $\mu\text{g}/\text{min}$ was administered intravenously to induce arrhythmia. For patients in whom no arrhythmia was induced even after this procedure, program stimulation and burst pacing were performed from the RV apex. A 3.5-mm irrigated-tip catheter (ThermoCool Navistar, Biosense-Webster) was used for mapping and ablation. A contact force-sensing catheter was used in three patients (TAPS group, case 7; MAPS group, cases 12 and 13). The local activation time was measured from the onset of the distal bipole of the mapping catheter to the earliest onset of the QRS complex in any of the 12 ECG leads. Based on ventricular activation during VA with multiple electrode catheters, a mapping catheter was inserted into the RV and/or the LV, and 3D activation mapping for VA was performed. For patients in whom arrhythmia originating in the LV was suspected, mapping of the LV was initiated after mapping the RV. When CT and MRI images were available, the 3D map was merged with CT and MRI images using intracardiac echocardiography. A tag indicating the AV annulus and His bundle locations on the 3D map was used to understand the anatomical position. The origin of the VA was identified by activation and pace mapping. The criteria for ablation were obtaining the earliest ventricular activation and/or pace map matching of 11/12 or more. RFCA was conducted with a setting of 25–30 W for 30 s per site. The indicators of successful ablation were defined as follows: loss of VA achieved with RFCA, no arrhythmia even after the discontinuation of RFCA, and no recurrence of VA even after isoproterenol loading and ventricular stimulation. The catheter position for the successful ablation site was recorded using fluoroscopy and 3D mapping. The anatomical position was examined using an electrogram, 3D mapping, and fluoroscopy. The definitions for the electrogram of the AV annulus were as follows: a simultaneous recording of atrial and ventricular electrograms of at least 0.05 and 0.5 mV, respectively, during sinus rhythm, and an A/V ratio of less than 1. The anatomical positions for both TAPS and MAPS were defined according to the classification of the attachment site of the accessory pathway [16]. The definitions of TAPS were as follows: a recording of AV annulus electrograms during sinus rhythm, the level of the CS ostium was the same as that of the posterior septum in the left anterior oblique (LAO) fluoroscopic view, and a location of 4–5 o'clock for the TA on the 3D mapping system. The definitions of MAPS were as follows: a recording of AV annulus electrograms during sinus rhythm, the same level of the CS ostium in the LAO fluoroscopic view, and a location of 7–8 o'clock for the mitral annulus on the 3D mapping system. The presence of complications during the perioperative period was evaluated.

2.4 Follow-up

Patients' ECGs were monitored for 48 h after the ablation and assessed for the recurrence of VA. Follow-up was performed for 6 months or more in the outpatient department to assess the recurrence of VA according to the patients' symptoms, 12-lead ECG, and ambulatory electrocardiography.

2.5 Statistical analysis

Continuous variables are expressed as mean \pm 1 standard deviation. For comparison of the continuous variables between the two groups, the Student's *t* test was conducted. For comparison of the nominal scale between the two groups, the Fisher's exact test was used. The statistical significance level in all the tests was set at $p = 0.05$. JMP pro 12.1.0 (SAS Institute Inc., Cary, NC) was used to perform statistical analysis.

3 Results

3.1 Clinical characteristics

The subjects consisted of 13 patients (eight men and five women) with VA originating in the posterior septum region (seven patients in the TAPS group; six patients in the MAPS group). Table 1 shows patient characteristics for both groups. One patient in the MAPS group had a history of syncope. The basic rhythm was sinus rhythm for all patients except patient 2. The QRS complex for the basic rhythm indicated LBBB in patient 9. Testing showed no signs of coronary artery disease in any of the patients. VA reduction was achieved with bisoprolol in patient 6. However, the other patients showed no clear efficacy of the drugs for VA.

3.2 ECG findings

Ten of the 13 patients presented with premature ventricular contraction (PVC), whereas two patients in the MAPS group and one in the TAPS group presented with non-sustained ventricular tachycardia. The 12-lead ECGs for both groups are shown in Figs. 1 and 2. The QRS complex for both groups showed superior axis deviation, LBBB ($n = 7$) and RBBB ($n = 6$) morphologies in lead V1. Among patients in both groups, nine had a precordial transition at \leq lead V3.

ECG characteristics in the TAPS group mainly showed a precordial transition for lead V4. However, there were two (29%) patients with precordial transition for lead V2 and one (14%) for lead V3. Rs and rS patterns were found in leads II and III, respectively. An R-wave larger than the S-wave in lead II was observed for five patients (71%). None of the patients in the TAPS group had a slurred initial part of the QRS complex in

the precordial leads based on Berruezo's criteria and MDI, except one patient who showed a pseudo delta wave ≥ 34 ms.

ECG for the MAPS group showed a precordial transition for lead V2 in all patients. Leads II and III primarily indicated the rS pattern. In the MAPS group, a slurred initial part of the QRS complex in the precordial lead was observed based on a pseudo delta wave in all patients. Five patients had an intrinsicoid deflection time ≥ 85 ms, three had MDI ≥ 0.55 , and none had the shortest RS complex ≥ 125 ms in either group.

Table 2 shows the results comparing each ECG characteristic between the two groups. MDI was significantly higher in the MAPS group (0.55 ± 0.05) than in the TAPS group (0.45 ± 0.04) ($p = 0.002$). The pseudo delta wave (23.9 ± 7.6 vs 45.3 ± 6.9 ; $p < 0.001$) and intrinsicoid deflection time (58.4 ± 24.5 vs 97.3 ± 16.5 , $p = 0.0071$) were significantly higher in the MAPS group than in the TAPS group. The R/S ratio in lead II was significantly higher in the TAPS group (2.78 ± 0.58) than in the MAPS group (0.50 ± 0.64) ($p = 0.029$). There was no significant difference between the two groups in the shortest RS complex (74.0 ± 20.52 vs 79.6 ± 13.8 ; $p = 0.58$), II/III amplitude ratio (0.86 ± 0.54 vs 0.55 ± 0.17 ; $p = 0.19$), and aVR/aVL amplitude ratio (0.71 ± 0.28 vs 0.50 ± 0.13 ; $p = 0.13$). The numbers of patients with a precordial transition for lead V2 and an s-wave in lead V6 were significantly higher in the MAPS group than in the TAPS group ($p = 0.029$).

The following ECG indicators were identified as characteristics predictive of MAPS: (1) the R/S ratio in lead II of 1 or less; (2) a precordial transition for lead V2; (3) an s-wave in lead V6; and (4) the presence of a slurred initial part of the QRS complex in the precordial leads ([4a] pseudo delta wave ≥ 34 ms; [4b] intrinsicoid deflection time ≥ 8 ms; and [4c] MDI ≥ 0.55). The sensitivity, specificity, and the positive (PPV) and negative (NPV) predictive values of these items are shown in Table 3. When patients who met criteria (1) to (3) were diagnosed as having MAPS-VA, the sensitivity, specificity, PPV, and NPV were 83.3, 100, 100, and 87.5%, respectively. All these values were 100% in patients who met at least two of the criteria from (1) to (3) and any of [4a] to [4c].

3.3 Electrophysiological study—mapping and ablation

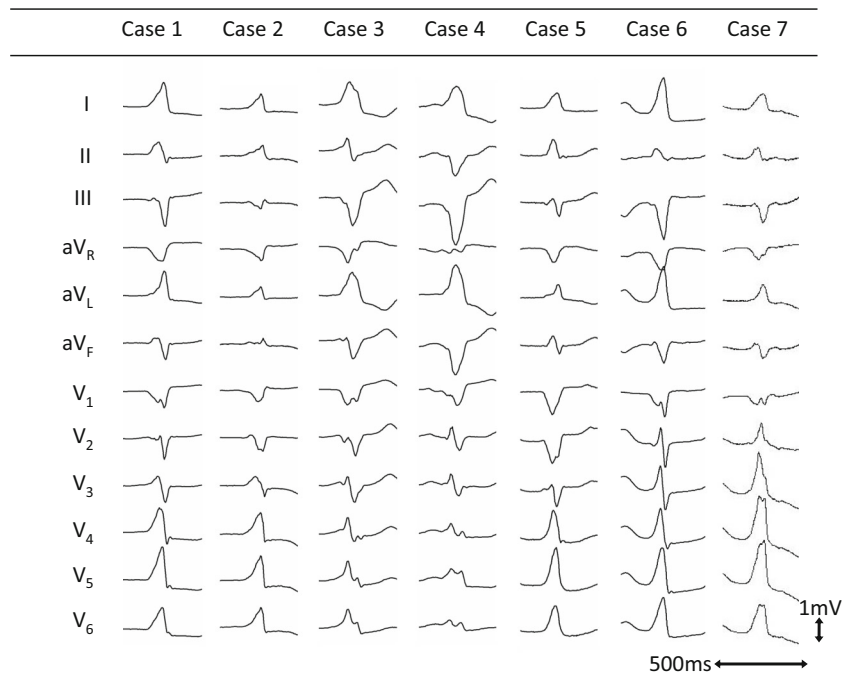
VA was induced spontaneously in all patients, except patient 10, in whom VA was induced after isoproterenol loading and ventricular pacing. In ventricular voltage mapping, none of the patients showed a low ventricular voltage area with a voltage < 1.5 mV, which would suggest a damaged myocardium. Seven patients underwent electroanatomical mapping with merged images from CT and MRI. Five patients underwent electroanatomical mapping using intra-cardiac echocardiography. All VAs were successfully ablated by four radiofrequency applications (interquartile range 1 to 8) for the posterior

Table 1 Patient and arrhythmia characteristics of TAPS group and MAPS group

	MAPS group												
	Case 1	Case 2	Case 3	Case 4	Case 5	Case 6	Case 7	Case 8	Case 9	Case 10	Case 11	Case 12	Case 13
Baseline													
Age	76	58	79	80	63	73	68	74	56	56	67	54	73
Gender	Male	Male	Female	Female	Male	Female	Male	Male	Male	Female	Male	Male	Female
Past history	HT, DM	DM	HT	HT	HT	HT	HT, HL	None	HT	None	HT	None	PE
LVEF, %	61	64	74	55	64	60	56	70	53	69	63	56	75
Symptom	Palpitation	Palpitation	Palpitation	Palpitation	Palpitation	Palpitation	Palpitation	Palpitation	Palpitation	Syncope	Palpitation	Palpitation	Palpitation
Medication	None	Bisoprolol	Propafenone	None	Carvedilol	Bisoprolol	None	Flisicainide	Mexiletine	Metoprolol	None	None	Metoprolol
Baseline ECG	SR	AF, Vp	SR	SR	SR	SR	SR	SR	SR, CLBBB	SR	SR	SR	SR, IRBBB
Evaluation of CAD	CAG, RI	CAG	CAG	CAG	UCG	CAG, RI	UCG	RI	CAG	CAG	Coronary CT	CAG	CAG
ECG of VA													
VA form	PVC	NSVT	PVC	PVC	PVC	NSVT	PVC	PVC	PVC	NSVT	PVC	PVC	PVC
LBBB/RBBB	LBBB	RBBB	LBBB	LBBB	LBBB	LBBB	RBBB	RBBB	LBBB	RBBB	RBBB	LBBB	RBBB
morphology													
Precordial transition	V4	V4	V4	V2	V4	V3	V2	V2	V2	V2	V2	V2	V2
Mapping/ablation													
LAT-QRS onset, ms	25	27	37	39	20	27	20	32	32	37	25	25	19
Pacemap score	11/12	11/12	12/12	11/12	11/12	12/12	12/12	12/12	12/12	12/12	11/12	11/12	12/12
Ablation site	RV	RV	RV	RV	RV	RV	RV	RV	RV (successful)	RV (successful)	RV (successful)	RV (successful)	RV (successful)
	(successful)	(successful)	(successful)	(successful)	(successful)	(successful)	(successful)	(successful)	(successful)	(successful)	(successful)	(successful)	(successful)
	ful)	ful)	ful)	ful)	ful)	ful)	ful)	ful)	ful)	ful)	ful)	ful)	ful)
Follow-up, months	7	63	7	38	6	6	6	14	17	6	8	12	6
Recurrence of VA	No	No	No	Yes	No	No	No	No	No	No	No	No	No

AF atrial fibrillation, CAD coronary artery disease, CAG coronary angiography, CLBBB complete left bundle branch block, CT computed tomography, DM diabetes mellitus, HT hypertension, IRBBB incomplete right bundle branch block, LAT local activation time, LBBB left bundle branch block, LV left ventricle, LVEF left ventricular ejection fraction, MAPS mitral annulus in the posterior septum, MCV middle cardiac vein, NSVT non-sustained ventricular tachycardia, PE pulmonary embolism, PVC premature ventricular contraction, RBBB right bundle branch block, RV radioisotope test, RV right ventricle, SR sinus rhythm, TAPS tricuspid annulus in the posterior septum, UCG ultrasound cardiography, VA ventricular arrhythmia, Vp ventricular pacing

Fig. 1 Twelve-lead electrocardiogram of QRS complexes during ventricular arrhythmia in the tricuspid annulus in the posterior septum group



septum. The local ventricular activation time recorded at the successful ablation site preceded the onset of the QRS complex by 27.9 ± 7.5 ms in the TAPS group and by 28.5 ± 6.6 ms in the MAPS group ($p = 0.87$). The local electrograms at the successful ablation sites fulfilled the criteria for AV annulus in all patients. The successful ablation sites on fluoroscopy and 3D mapping were found in the posterior septal portion of the AV annulus at the level of the CS ostium in all patients. Figure 3 and Fig. 4 show the local electrograms, fluoroscopic

view, and 3D map at the successful ablation sites for patients 7 and 9. In the MAPS group, the local electrograms preceded the onset of the QRS complex by 13.5 ± 3.5 ms in the posterior septal region of the RV and by 12.8 ± 5.1 ms in the proximal CS. In the TAPS group, mapping was not performed in the posterior septal region of the LV. Regarding complications, transient complete AV block was observed in patient 6 during radiofrequency application, but no perioperative complications were found in the other patients.

Fig. 2 Twelve-lead electrocardiogram of QRS complexes during ventricular arrhythmia in the mitral annulus in the posterior septum group

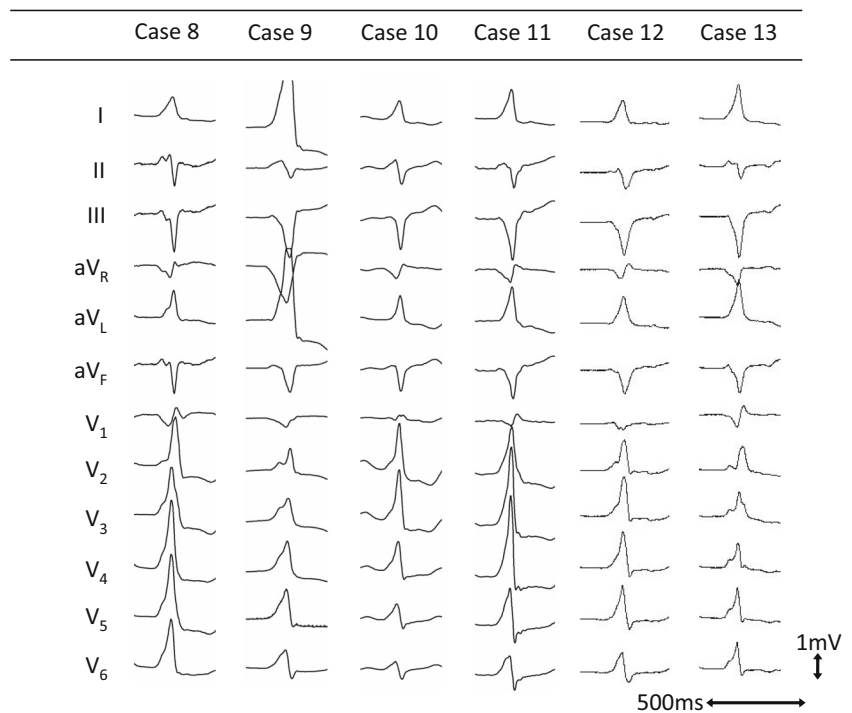


Table 2 Comparison of electrocardiographic characteristics between TAPS group and MAPS group

	TAPS group	MAPS group	<i>p</i> value (* <i>p</i> < 0.05)
QRS duration, ms	138.4 ± 7.6	143.2 ± 9.9	0.35
II R/S ratio	2.78 ± 0.58	0.50 ± 0.64	0.029*
II/III amplitude ratio	0.86 ± 0.54	0.55 ± 0.17	0.19
aVR/aVL amplitude ratio	0.71 ± 0.28	0.50 ± 0.13	0.13
V2 transition (%)	2 (29)	6 (86)	0.021*
s-wave in V6 (%)	1 (14)	5 (83)	0.029*
Pseudo delta wave, ms	23.9 ± 7.6	45.3 ± 6.9	< 0.001*
Intrinsicoid deflection time, ms	58.4 ± 24.5	97.3 ± 16.5	0.007*
Shortest RS complex, ms	74.0 ± 20.52	79.6 ± 13.8	0.58
MDI	0.45 ± 0.04	0.55 ± 0.05	0.002*

TAPS tricuspid annulus in the posterior septum, MAPS mitral annulus in the posterior septum, MDI maximum deflection index

3.4 Follow-up

The patients were followed up for 7 (interquartile range 6 to 15.5) months. PVC recurred in patient 4 one month after discharge. The remaining 12 patients showed no recurrence according to the symptoms, ECG, and ambulatory ECG.

4 Discussion

4.1 Main findings

This study highlights the ECG characteristics of TAPS-VA and MAPS-VA. The QRS complex for VA showed superior axis deviation, and LBBB and RBBB morphologies with relatively early precordial transition in each group. Four ECG characteristics were identified that predicted MAPS-VA. It was possible to characterize patients who met at least two of criteria (1) to (3) and any of the criteria [4a] to [4c] as having MAPS-VA, with a diagnostic sensitivity and specificity of 100%. Although RFCA was successful in all 13 patients during the acute phase, 1

patient in the TAPS group experienced recurrence of VA during the late phase after RFCA.

4.2 Anatomy around the ventricular posterior septum and its electrophysiological importance

The area around the ventricular posterior septum is an important region electrophysiologically because it contains many anatomical structures that may be arrhythmogenic. Anatomically, the ventricular posterior septum is a part of the trigonal pyramidal region consisting of a summit with the membranous septum and a base with the epicardium of the cardiac crux, i.e., the so-called inferior pyramidal space [17]. The two sides of the trigonal pyramid consist of the right and left atria, and the other side is formed by a complex of the muscular septum of the LV and the PSP of the LV. The plane of the TA is displaced by 0.5 to 1.0 cm inferiorly and apically relative to the plane of the MA. Therefore, the crest of the muscular ventricular septum contacts the right atrium (RA) directly. The posterior septal area, which has been conventionally used in cardiac electrophysiology, is the inferior part of the inferior pyramidal space anatomically. Since the CS ostium is positioned at the inferior part of the inferior pyramidal space, the level of the

Table 3 Sensitivity, specificity, and positive and negative predictive values of electrocardiographic characteristics for predicting ventricular arrhythmia arising from MAPS

ECG characteristics (<i>n</i>)	Prediction	Sensitivity (%)	Specificity (%)	PPV (%)	NPV (%)
(1) II R/S < 1 (8)	MAPS	100	71	75	100
(2) V2 transition (8)	MAPS	100	71	75	100
(3) s-wave in V6 (6)	MAPS	83	85	83	46
[4a] Pseudo delta wave ≥ 34 ms (7)	MAPS	100	85	86	100
[4b] Intrinsicoid deflection time ≥ 85 ms (5)	MAPS	83	100	100	88
[4c] MDI ≥ 0.55 (3)	MAPS	50	100	100	70
All of (1)–(3) (5)	MAPS	83	100	100	88
(1)–(3) ≥ 2 and any of [4a]–[4c] (6)	MAPS	100	100	100	100

MAPS mitral annulus in the posterior septum, MDI maximum deflection index, NPV negative predictive value, PPV positive predictive value

Fig. 3 Patient 7 in the tricuspid annulus in the posterior septum group. **a** Pace mapping and local electrocardiogram of the successful ablation site. The local ventricular electrogram preceded the QRS onset by 20 ms during PVC. **b** The red tag (arrow) indicates the successful ablation site on the 3D mapping system. The 3D mapping system is merged with CT image. The CT image of the left atria is removed for clarity. **c** Fluoroscopic views of the ablation catheter at the successful ablation site. 3D, three-dimensional; ABL, ablation catheter; CT, computed tomography; CS, coronary sinus; LAO, left anterior oblique; PVC, premature ventricular contraction; RAO, right anterior oblique; SR, sinus rhythm; uni, unipolar

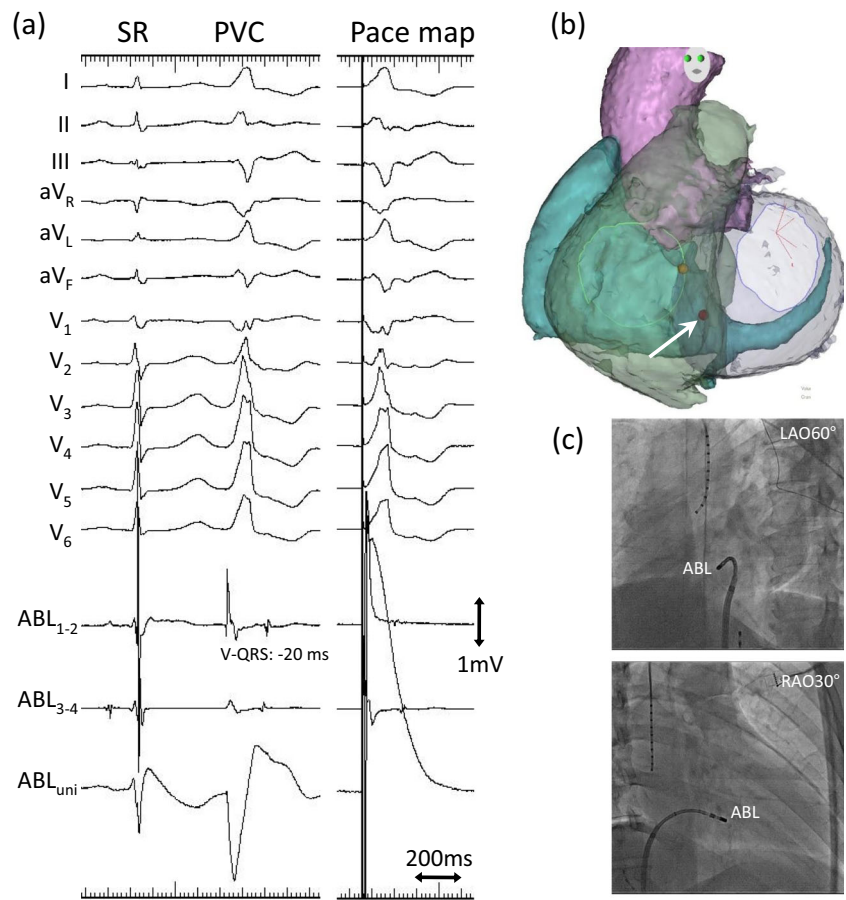
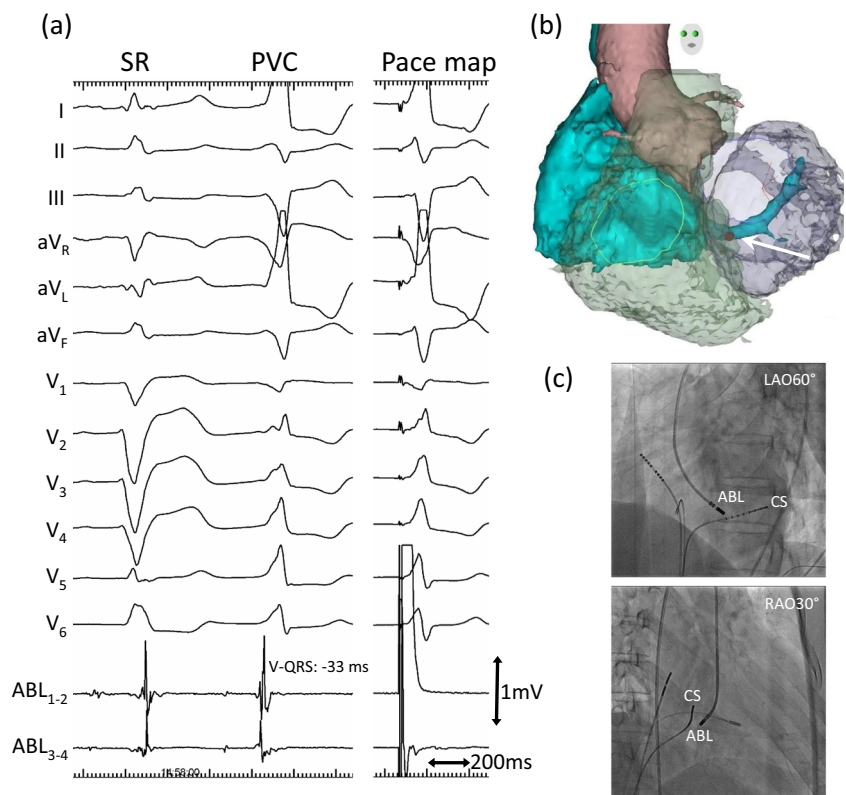


Fig. 4 Patient 9 in the mitral annulus in the posterior septum group. **a** Pace mapping and local electrocardiogram of the successful ablation site. The local ventricular electrogram preceded the QRS onset by 33 ms during PVC. **b** The red tag (arrow) indicates the successful ablation site on the 3D mapping system. The 3D mapping system is merged with CT image. The CT image of the left atria is removed for clarity. **c** Fluoroscopic views of the ablation catheter at the successful ablation site. 3D, three-dimensional; ABL, ablation catheter; CT, computed tomography; CS, coronary sinus; LAO, left anterior oblique; PVC, premature ventricular contraction; RAO, right anterior oblique; SR, sinus rhythm; uni, unipolar



CS ostium is the same as that of the posterior septum of the ventricle on LAO fluoroscopic projection.

Electrophysiologically, the TA in the septal region is classified into three regions: the anterior septal region, mid septal region, and posterior septal region [16]. The His bundle is located in the anterior septal region of the TA. Idiopathic VA originating in the vicinity of the His bundle arises from both the TA anterior septal region and the TA mid septal region [18]. The His bundle penetrates the membranous septum and continues as a branching portion. The left posterior fascicle runs through the ventricular inferior septum in the direction of the apex. Various arrhythmias occur based on these anatomical structures around the ventricular inferior septum. The most common form of idiopathic left ventricular tachycardia arises from the left posterior fascicle region [19]. VA originating in the cardiac crux on the epicardium side has been reported [8, 9], and VA originating in the PSP of the LV, which can be ablated from the RA, was recently reported [10]. Since the anatomical locations of these VAs are close to the TAPS and MAPS regions, the 12-lead ECG findings of these VAs resemble those of TAPS-VA and MAPS-VA. The diagnosis of VA by 12-lead ECG is important to ablate VA originating from the ventricular posterior/inferior septum region.

4.3 Electrocardiographic characteristics and presumed mechanism in the TAPS and MAPS groups

In the TAPS group, the QRS complex of VA showed superior axis deviation and LBBB and RBBB morphologies with relatively early precordial transition. Precordial transition was most commonly found in lead V4. However, there were two patients (29%) with precordial transition in lead V2 and one patient (14%) with precordial transition in lead V3. It was notable that the precordial transition of the TAPS-VA was relatively early, despite the origins within the RV. Lead II primarily showed an Rs pattern, while lead III showed an rS pattern. Tada et al. [3] reported that VA originating in the TA accounted for approximately 8% of idiopathic VA. VA arising from the TA in the septal region accounted for approximately 74%, and that in the free wall region accounted for 26% of all VAs arising from the TA. In the study by Tada et al. [3], VA arising from the TA in the posterior septal regions showed LBBB or RBBB morphology in lead V1, and a precordial transition in lead V3 or earlier. In the present study, two patients in the TAPS group who had the precordial transition in lead V2 needed to be differentiated from those with VA originating in the LV. Leads II and III are thought to be useful for classifying the localization around the TA. Leads II and III have positive polarity in the anterior septal region and negative polarity in the posterior region [3, 18]. In the TAPS group, R/S ratio > 1 in lead II was found in five patients (71%). In TAPS-VA, it is presumed that activation of the ventricular posterior septum propagates downward and leftward, which

is parallel to lead II, causing the higher initial R-wave in lead II than in MAPS-VA. There have been no reports describing a slurred initial part of the QRS complex in VA originating in the TA. Our study showed that no patient in the TAPS group had a slurred initial part of the QRS complex in precordial leads based on Berruezo's criteria and MDI, except one patient who showed a pseudo delta wave ≥ 34 ms.

In the MAPS group, the QRS complex of VA had LBBB or RBBB morphology in lead V1 and superior axis deviation. Precordial transition was observed in lead V2 in all patients. Lead II primarily showed an rS pattern, while lead III showed rS or QS patterns. Tada et al. [5] reported 19 patients with VA originating in the MA. In their study, the most common VA origin site was the anterior region (58%), followed by the posterior septum region (31%) and posterior region (11%). The inferior leads showed positive polarity for the anterior region and negative polarity for the posterior septum or posterior region. For the precordial transition, only VA originating in the septal region was observed in lead V2, and other regions showed no transitions. Tada et al. [5] reported that six patients in the posterior septum group showed QS and rS patterns in leads II/III. In the MAPS group, lead II primarily showed an rS pattern, while lead III showed rS or QS patterns, which is consistent with that reported by Tada et al. [5]. Compared with the TAPS group, the MAPS group showed a significantly lower R/S ratio in lead II (2.78 ± 0.58 vs 0.50 ± 0.64 ; $p = 0.029$).

The percentages of an s-wave in lead V6 were 8% [3] among patients with VA originating in the TA and 92% among patients with VA originating in the MA, with the exception of the anterior region of the MA [7]. Additionally, an s-wave in lead V6 was more common in the MAPS group than the TAPS group (14 vs 83%; $p = 0.025$), and this finding was useful for differentiating patients with MAPS-VA from those with TAPS-VA. An s-wave in lead V6 reflects the excitation of the ventricular septum and the RV; therefore, an s-wave in lead V6 appears when the ventricular septum and the RV are excited later than the free wall of the LV. The presence of an s-wave in lead V6 is consistent with LV outflow arrhythmia, which is useful for differentiating idiopathic RV outflow tract arrhythmia [11]. Similarly, an s-wave in lead V6 was useful for distinguishing between the RV and LV in patients with VA originating in the posterior septum.

In the present study, we identified a set of ECG diagnostic criteria with excellent sensitivity and specificity to distinguish MAPS-VA from TAPS-VA because we included the criterion that MAPS-VA has a slurred initial part of the QRS complex in the precordial leads. Kumagai et al. [7] reported a delta wave-like morphology of ECG of VA originating in the MA. In their report [7], the intrinsicoid deflection time was 99 ± 13 ms, which is similar to the result for the MAPS group in our study (97 ± 16 ms). According to Kumagai et al. [7], since the delta wave and the intrinsicoid deflection time are indicators of arrhythmia originating in the epicardium side, the origin of

VA arising from the MA may be deep inside the subendocardium or epicardium. Anatomically, the epicardial side of the ventricular posterior septal region is the cardiac crux. The ECG characteristics of VA originating in the cardiac crux include the following: (1) negative delta wave in inferior leads, (2) positive QRS complex in leads V2–V6, (3) MDI ≥ 0.55 , (4) prominent R-wave in lead V2 [8], and (5) QS pattern in lead V1 [9]. Regarding the ECG of the MAPS group, findings (2) to (4) were consistent with MAPS, but the MAPS group had an r-wave in the initial component of lead II and various QRS morphologies (including R, qR, and rS patterns) in lead V1, which was not consistent with findings (1) and (5). Bazan et al. [20] compared the QRS morphologies during pace mapping from endocardial and epicardial sites of the LV. At the basal inferior region of the LV, the r-wave was identified as an initial component of the QRS complex of inferior leads through endocardium pacing, and the QS pattern in inferior leads was identified through epicardial pacing. Based on the findings of Bazan et al. [20], the initial r-wave in lead II in the MAPS group may suggest that the origin of VA is the endocardial side of the posterior septum. The reason that the MAPS group had a slurred initial part of the QRS complex in the precordial leads despite an origin on the endocardial side was thought to be the fact that the myocardial wall thickness of MAPS region [21] is larger than that of the TAPS region [22]. A thicker wall could produce the more anisotropic conduction that is associated with the initial precordial slurring. During the actual ablation procedure in the MAPS group, we found that the slurred initial part of the QRS complex in the precordial leads for PVC disappeared when ablation to the MAPS region was repeated. This finding supports the hypothesis that the myocardial mass in the MAPS region is involved in slur formation.

The VA arising from PSP of the LV (PSP-VA), which was ablated from RA under intra-cardiac echocardiography, has been reported by Santangeli et al. [10]. The ECG waveform of PSP-VA had a slurred initial part of the precordial leads, and the group exhibiting an RBBB with a left superior axis had similar ECG characteristics to those of the MAPS group. This group of PSP-VA met three of our criteria ([1] R < S wave in lead II, [2] s-wave in lead V6, and [3] slurred initial part of the QRS complex in the precordial leads), and it would be diagnosed as belonging to the MAPS group. Although it is necessary to examine a large number of ECG waveforms of PSP-VA, it has the characteristics of MAPS. If ablation for MAPS is ineffective, the RA approach under intra-cardiac echocardiography guidance may be required.

4.4 Catheter ablation

Since successful treatment was achieved in both groups during the acute and late phases, RFCA for VA originating in the posterior septum was considered effective. One patient in the

TAPS group experienced recurrence during the late phase. The treatment outcome of VA arising from the TA in the septal region was reported to be inferior to that from TA in the free wall region [3]. The recurrence was attributed to poor fixation of the ablation catheter to the TAPS region, leading to inadequate ablation. To improve the stability of catheter ablation, a long guiding sheath should be used during ablation of the TAPS region. Regarding complications, transient complete AV block was observed in patient 6. In patient 6, the His bundle potential recording site was lower than usual, and transient atrioventricular block was observed by the site of ablation before successful ablation. The causes of the occurrence of transient atrioventricular block in this case may have been as follows: the catheter was not fixed enough because a long guiding sheath was not used and the His bundle potential recording site was anatomically low because of enlargement of the ascending aorta.

4.5 Limitations

There are several limitations to this study. First, since a rare type of arrhythmia was examined, the sample size was small. VA originating in the ventricular posterior septum accounts for < 30% of all AV annular VAs. The sensitivity and specificity of our diagnostic criteria are expected to change in a larger study with more participants, but the consistency of our criteria would be maintained. Second, since precordial transition would be influenced by cardiac rotation, it is necessary to assess the precordial transition of the basic rhythm. This study included patients with pacing rhythm issues and one patient with LBBB, but the total number of participants was small. Therefore, we could not consider cardiac rotation. Third, since no left-sided mapping was performed in the TAPS group, the precedence of local ventricular activation of the LV could not be assessed. Fourth, since we had no case of VA of the basal crux in our series, we could not directly compare the 12-lead ECG waveform of VA of the basal crux, TAPS-VA, and MAPS-VA. Therefore, we referred to previous reports [8, 9] about the 12-lead ECG waveform of VA of the basal crux. Further study of the direct comparison of the 12-lead ECG waveforms of the TAPS group, MAPS group, and basal crux group is required.

5 Conclusions

VA arising from the AV annulus in the posterior septal region has superior axis deviation, and LBBB and RBBB morphologies with relatively early precordial transition. Based on the four ECG characteristics, it is possible to differentiate MAPS-VA from TAPS-VA. The results of such differentiation may be useful for treatment involving catheter ablation for the ventricular posterior septum.

Compliance with ethical standards

Conflict of interest The authors declare that they have no conflict of interest.

Ethical approval All procedures performed in studies involving human participants were in accordance with the ethical standards of the institutional and/or national research committee and with the 1964 Helsinki declaration and its later amendments or comparable ethical standards. This study was performed after obtaining approval from the institution's ethical committee.

Informed consent Informed consent was obtained from all individual participants included in this study.

References

- Stevenson WG, Soejima K. Catheter ablation for ventricular tachycardia. *Circulation*. 2007;115(21):2750–60. <https://doi.org/10.1161/CIRCULATIONAHA.106.655720>.
- Yamada T, Kay GN. Optimal ablation strategies for different types of ventricular tachycardias. *Nat Rev Cardiol*. 2012;9(9):512–25. <https://doi.org/10.1038/nrcardio.2012.74>.
- Tada H, Tadokoro K, Ito S, Naito S, Hashimoto T, Kaseno K, et al. Idiopathic ventricular arrhythmias originating from the tricuspid annulus: prevalence, electrocardiographic characteristics, and results of radiofrequency catheter ablation. *Heart Rhythm*. 2007;4(1):7–16. <https://doi.org/10.1016/j.hrthm.2006.09.025>.
- Van Herendael H, Garcia F, Lin D, Riley M, Bala R, Cooper J, et al. Idiopathic right ventricular arrhythmias not arising from the outflow tract: prevalence, electrocardiographic characteristics, and outcome of catheter ablation. *Heart Rhythm*. 2011;8(4):511–8. <https://doi.org/10.1016/j.hrthm.2010.11.044>.
- Tada H, Ito S, Naito S, Kurosaki K, Kubota S, Sugiyasu A, et al. Idiopathic ventricular arrhythmia arising from the mitral annulus: a distinct subgroup of idiopathic ventricular arrhythmias. *J Am Coll Cardiol*. 2005;45(6):877–86. <https://doi.org/10.1016/j.jacc.2004.12.025>.
- Wasmer K, Kobe J, Decherer DG, Bittner A, Pott C, Monnig G, et al. Ventricular arrhythmias from the mitral annulus: patient characteristics, electrophysiological findings, ablation, and prognosis. *Heart Rhythm*. 2013;10(6):783–8. <https://doi.org/10.1016/j.hrthm.2013.02.007>.
- Kumagai K, Yamauchi Y, Takahashi A, Yokoyama Y, Sekiguchi Y, Watanabe J, et al. Idiopathic left ventricular tachycardia originating from the mitral annulus. *J Cardiovasc Electrophysiol*. 2005;16(10):1029–36. <https://doi.org/10.1111/j.1540-8167.2005.40749.x>.
- Doppalapudi H, Yamada T, Ramaswamy K, Ahn J, Kay GN. Idiopathic focal epicardial ventricular tachycardia originating from the crux of the heart. *Heart Rhythm*. 2009;6(1):44–50. <https://doi.org/10.1016/j.hrthm.2008.09.029>.
- Kawamura M, Gerstenfeld EP, Vedantham V, Rodrigues DM, Burkhardt JD, Kobayashi Y, et al. Idiopathic ventricular arrhythmia originating from the cardiac crux or inferior septum: epicardial idiopathic ventricular arrhythmia. *Circ Arrhythm Electrophysiol*. 2014;7(6):1152–8. <https://doi.org/10.1161/CIRCEP.114.001704>.
- Santangeli P, Hutchinson MD, Supple GE, Callans DJ, Marchlinski FE, Garcia FC. Right atrial approach for ablation of ventricular arrhythmias arising from the left posterior-superior process of the left ventricle. *Circ Arrhythm Electrophysiol*. 2016;9(7):e004048. <https://doi.org/10.1161/CIRCEP.116.004048>.
- Ito S, Tada H, Naito S, Kurosaki K, Ueda M, Hoshizaki H, et al. Development and validation of an ECG algorithm for identifying the optimal ablation site for idiopathic ventricular outflow tract tachycardia. *J Cardiovasc Electrophysiol*. 2003;14(12):1280–6.
- Yoshida N, Yamada T, McElderry HT, Inden Y, Shimano M, Murohara T, et al. A novel electrocardiographic criterion for differentiating a left from right ventricular outflow tract tachycardia origin: the V2S/V3R index. *J Cardiovasc Electrophysiol*. 2014;25(7):747–53. <https://doi.org/10.1111/jce.12392>.
- Efimova E, Dinov B, Acou WJ, Schirripa V, Kornej J, Kosiuk J, et al. Differentiating the origin of outflow tract ventricular arrhythmia using a simple, novel approach. *Heart Rhythm*. 2015;12(7):1534–40. <https://doi.org/10.1016/j.hrthm.2015.04.004>.
- Berruezo A, Mont L, Nava S, Chueca E, Bartholomay E, Brugada J. Electrocardiographic recognition of the epicardial origin of ventricular tachycardias. *Circulation*. 2004;109(15):1842–7. <https://doi.org/10.1161/01.CIR.0000125525.04081.4B>.
- Daniels DV, Lu YY, Morton JB, Santucci PA, Akar JG, Green A, et al. Idiopathic epicardial left ventricular tachycardia originating remote from the sinus of Valsalva: electrophysiological characteristics, catheter ablation, and identification from the 12-lead electrocardiogram. *Circulation*. 2006;113(13):1659–66. <https://doi.org/10.1161/CIRCULATIONAHA.105.611640>.
- Arruda MS, McClelland JH, Wang X, Beckman KJ, Widman LE, Gonzalez MD, et al. Development and validation of an ECG algorithm for identifying accessory pathway ablation site in Wolff-Parkinson-White syndrome. *J Cardiovasc Electrophysiol*. 1998;9(1):2–12.
- Mori S, Fukuzawa K, Takaya T, Takamine S, Ito T, Fujiwara S, et al. Clinical structural anatomy of the inferior pyramidal space reconstructed within the cardiac contour using multidetector-row computed tomography. *J Cardiovasc Electrophysiol*. 2015;26(7):705–12. <https://doi.org/10.1111/jce.12687>.
- Komatsu Y, Taniguchi H, Miyazaki S, Kusa S, Takayama K, Kakita K, et al. Two distinct electrocardiographic forms of idiopathic ventricular arrhythmia originating in the vicinity of the His bundle. *Europace*. 2012;14(12):1778–85. <https://doi.org/10.1093/europace/eus160>.
- Nogami A. Purkinje-related arrhythmias. *J Arrhythmia*. 2011;27(1):6–27. [https://doi.org/10.1016/s1880-4276\(11\)80004-9](https://doi.org/10.1016/s1880-4276(11)80004-9).
- Bazan V, Gerstenfeld EP, Garcia FC, Bala R, Rivas N, Dixit S, et al. Site-specific twelve-lead ECG features to identify an epicardial origin for left ventricular tachycardia in the absence of myocardial infarction. *Heart Rhythm*. 2007;4(11):1403–10. <https://doi.org/10.1016/j.hrthm.2007.07.004>.
- Dawson DK, Maceira AM, Raj VJ, Graham C, Pennell DJ, Kilner PJ. Regional thicknesses and thickening of compacted and trabeculated myocardial layers of the normal left ventricle studied by cardiovascular magnetic resonance. *Circ Cardiovasc Imaging*. 2011;4(2):139–46. <https://doi.org/10.1161/CIRCIMAGING.110.960229>.
- Ho SY, Nihoyannopoulos P. Anatomy, echocardiography, and normal right ventricular dimensions. *Heart*. 2006;92(Suppl 1):i2–13. <https://doi.org/10.1136/hrt.2005.077875>.